

ORIGINAL ARTICLE

Upregulation of Fc γ RIIB by resveratrol via NF- κ B activation reduces B-cell numbers and ameliorates lupus

Jyun-Pei Jhou, Se-Jie Chen, Ho-Yin Huang, Wan-Wan Lin, Duen-Yi Huang and Shiang-Jong Tzeng

Resveratrol, an anti-inflammatory agent, can inhibit pro-inflammatory mediators by activating Sirt1, which is a class III histone deacetylase. However, whether resveratrol can regulate inhibitory or anti-inflammatory molecules has been less studied. Fc γ RIIB, a receptor for IgG, is an essential inhibitory receptor of B cells for blocking B-cell receptor-mediated activation and for directly inducing apoptosis of B cells. Because mice deficient in either Sirt1 or Fc γ RIIB develop lupus-like diseases, we investigated whether resveratrol can alleviate lupus through Fc γ RIIB. We found that resveratrol enhanced the expression of Fc γ RIIB in B cells, resulting in a marked depletion of plasma cells in the spleen and notably in the bone marrow, thereby decreasing serum autoantibody titers in MRL/lpr mice. The upregulation of Fc γ RIIB by resveratrol involved an increase of Sirt1 protein and deacetylation of p65 NF- κ B (K310). Moreover, increased binding of phosphor-p65 NF- κ B (S536) but decreased association of acetylated p65 NF- κ B (K310) and phosphor-p65 NF- κ B (S468) to the -480 promoter region of *Fcgr2b* gene was responsible for the resveratrol-mediated enhancement of Fc γ RIIB gene transcription. Consequently, B cells, especially plasma cells, were considerably reduced in MRL/lpr mice, leading to improvement of nephritis and prolonged survival. Taken together, we provide evidence that pharmacological upregulation of Fc γ RIIB expression in B cells via resveratrol can selectively reduce B cells, decrease serum autoantibodies and ameliorate lupus nephritis. Our findings lead us to propose Fc γ RIIB as a new target for therapeutic exploitation, particularly for lupus patients whose Fc γ RIIB expression levels in B cells are downregulated.

Experimental & Molecular Medicine (2017) 49, e381; doi:10.1038/emm.2017.144; published online 29 September 2017

INTRODUCTION

Systemic lupus erythematosus (SLE) is an autoimmune disease that predominantly affects young females.¹ Patients with SLE gradually develop lupus nephritis owing to tissue damage and chronic inflammation resulting from the deposition of excess immune complexes (ICs). Without proper treatment, patients can eventually die of renal failure. To date, no therapy for SLE has been satisfactory. The current standard of care for SLE patients mainly relies on corticosteroids, which essentially induce systemic immunosuppression to control the disease. However, the use of corticosteroids by patients is a double-edged sword because of its severe side effects, including infection and long-term metabolic imbalance.² These problems highlight an unmet medical need for SLE patients and warrant the development of new, more effective therapies. Recently, it has been demonstrated that treatment of lupus-prone MRL/lpr mice with panobinostat, an inhibitor of classes I, II and IV histone deacetylases (HDACs), can selectively reduce the

number of autoreactive B cells, leading to an alleviation of lupus nephritis. The molecular basis of how a HDAC can influence B cells remains to be determined;³ however, B cells have acquired increasing attention as chief contributors and important therapeutic targets of autoimmune diseases, including SLE.⁴

Resveratrol (3,4',5-trihydroxy-*trans*-stilbene) is a small polyphenol of the stilbenoid class. In response to environmental stresses, resveratrol is produced by various plants, including grapes, peanuts and berries.^{5,6} Many studies have demonstrated that resveratrol can protect against inflammation, oxidative stress and tumorigenesis. The beneficial effects of resveratrol have been attributed to anti-inflammatory and pro-apoptotic properties mediated by Sirt1 (sirtuin 1), an NAD⁺-dependent deacetylase that belongs to the class III HDAC family.⁷ Resveratrol is an activator of Sirt1, which can induce the deacetylation of substrates to modulate their activities. Resveratrol can inhibit p65 NF- κ B, peroxisome proliferator-activated

Department of Pharmacology, College of Medicine, National Taiwan University, Taipei, Taiwan

Correspondence: Professor S-J Tzeng, Department of Pharmacology, College of Medicine, National Taiwan University, Room 1118, No. 1, Section 1, Ren-Ai Road, Taipei 10051, Taiwan.

E-mail: sjtzeng@ntu.edu.tw

Received 12 October 2016; revised 22 March 2017; accepted 29 March 2017

receptor α and cyclooxygenase 2, and it upregulates eNOS and p53 to promote apoptosis of tumor cells.⁸ To date, limited studies have suggested a link between Sirt1 and SLE development. Sirt1 deficiency in mice results in the development of a lupus-like disease, which is manifested by a high titer of serum anti-nuclear antibodies (Abs) and chronic glomerulonephritis.⁹ In CD4⁺ T cells of active SLE patients, histone modifications appear abnormal, and Sirt1 mRNA levels are significantly increased, suggesting adaptive changes of Sirt1 in SLE patients.¹⁰ Moreover, Sirt1 promoter polymorphisms can modify SLE morbidity, with the rs3758391 T allele being a risk factor for nephritis and a higher SLE disease activity index.¹¹ Currently, it remains to be elucidated how Sirt1 functionally influences SLE severity.

Fc γ RIIB is an inhibitory Fc γ receptor that binds the Fc portion of its ligand IgG. The best known function of Fc γ RIIB is to regulate serum Ab levels via a negative feedback loop, inhibiting B cells when sufficient Abs are made.^{12,13} When Fc γ RIIB and BCR are co-engaged by ICs, the ITIM in the cytoplasmic domain of Fc γ RIIB is phosphorylated by Lyn kinase to allow the recruitment of SHIP to initiate downstream signaling pathways, thereby blocking B-cell activation.^{14,15} Meanwhile, we have recently shown that Fc γ RIIB can directly trigger the apoptosis of B cells via a c-Abl-dependent pathway independently of the BCR.^{16,17} Thus, in the presence of IgG ICs, Fc γ RIIB can transduce two distinct inhibitory signals that are determined by the affinity of antigen (Ag) to the BCR. The critical role of Fc γ RIIB in B cells can be demonstrated in Fc γ RIIB-deficient mice, which display a lupus-like disease, with massive expansion of splenic plasma cells (PCs) and excess IC deposition in the kidneys.¹⁸ Consistent with these findings, Fc γ RIIB expression in B cells of lupus-prone mice is often downregulated and thereby obviates inhibition.¹⁹ In humans, the Fc γ RIIB locus has been identified as a susceptibility allele of SLE across populations.^{12,20} Moreover, the expression levels of Fc γ RIIB on memory B cells and PCs, but not macrophages, are considerably decreased in patients with SLE.^{21–23} We recently showed that human PCs express higher Fc γ RIIB on the cell surface than memory and naive B cells in the circulation. Accordingly, the PCs are most sensitive to apoptosis triggered by Fc γ RIIB.¹⁷ These results strongly support a crucial role for Fc γ RIIB in the control of PC numbers to maintain homeostasis of serum Ab levels.^{17,24,25}

Given that Sirt1 and Fc γ RIIB might act concertedly for anti-inflammation, we were interested in understanding their relationship with respect to SLE disease development and their potential for therapeutic exploitation. To this end, we used resveratrol to activate Sirt1 and determine its therapeutic benefits in MRL/*lpr* mice. As previously reported, the lupus onset and flare of MRL/*lpr* mice are driven by Th1 cells owing to a spontaneous *fas* mutation, which results in a defect in the Fas-dependent deletion of autoreactive T cells.²⁶ Therefore, MRL/*lpr* mice can enable us to determine whether resveratrol selectively eliminates B cells when pathogenic T cells persist. In addition, the potential link between resveratrol and Fc γ RIIB in B cells can be addressed.

MATERIALS AND METHODS

Reagents

Resveratrol ($\geq 99\%$ pure), olive oil (highly refined, low acidity) and DMSO were purchased from Sigma-Aldrich (St Louis, MO, USA). F(ab')₂ fragment of goat anti-mouse IgG, μ -chain-specific goat anti-mouse IgM, and rabbit peroxidase-anti-peroxidase ICs were purchased from Jackson ImmunoResearch Laboratories (West Grove, PA, USA). Mouse mAb specific for CD19-PE-Cy7 (clone 1D3) was obtained from eBioscience (San Diego, CA, USA). Mouse IgG isotypes and mAbs specific to CD16/32 (clone 2.4G2), CD138-BV421 (clone 281-2), CD11b-PerCP-Cy5.5 (clone M1/70), CD11c-AlexaFluor 700 (clone HL3) and GL7-AlexaFluor 647 (clone GL7) were acquired from BD Biosciences (San Jose, CA, USA). Mouse IgM isotype Ab was obtained from SouthernBiotech (Birmingham, AL, USA). Ninety-six-well MultiScreen HTS filter plates were acquired from Merck Millipore (Billerica, MA, USA). Blood lancet was obtained from MEDipoint (Mineola, NY, USA). Vectastain ABC kits packed with biotinylated goat anti-rabbit IgG, rabbit anti-goat IgG and rabbit anti-rat IgG mAbs were purchased from Vector Laboratories (Burlingame, CA, USA). Abs specific to mouse B220, Fc γ RIIB, and phosphor-c-Abl (Y245) were obtained from Santa Cruz Biotechnology (Dallas, TX, USA). Urine analysis strips were acquired from Macheray-Nagel (Duren, Germany).

Mice

MRL/*lpr* mice were maintained in specific pathogen-free conditions at the Center for Laboratory Animals of the College of Medicine of National Taiwan University. The MRL/*lpr* mice were obtained from the Jackson Laboratory. The protocols of animal use were reviewed and the experiments performed according to the guidelines approved by the Institutional Animal Care and Use Committee (IACUC) of the College of Medicine of National Taiwan University (protocol number: 20120483). Seventeen-week-old female mice were divided into two groups, and they received 10 intra-peritoneal injections of either vehicle (olive oil) or 20 mg kg⁻¹ per day resveratrol every other day. Olive oil was used to enhance the solubility and bioavailability of resveratrol. The survival rate of mice was monitored and documented after the initiation of treatment for 6 weeks.

Flow cytometry

Cells were stained with FITC-conjugated anti-CD32 mAbs at 4 °C for 10 min, followed by incubation with the following mAbs: CD138-BV421, CD19-PE-Cy7, CD11b-PerCP-Cy5.5, CD11c-AlexaFluor 700 and GL7-AlexaFluor 647 for 20 min. Dead cells were stained with 7-aminoactinomycin D (7-AAD) and annexin V (Biolegend, San Diego, CA, USA) before using an LSRFortessa (BD Biosciences) for multi-color flow cytometry. The data were analyzed using FlowJo, version 7.6 (FLOWJO, Ashland, OR, USA).

Enzyme-linked immunosorbent assay

Five μ g ml⁻¹ of either mouse μ chain- or γ chain-specific Abs were added into wells of 96-well plates to incubate at 4 °C overnight. To detect anti-dsDNA autoantibodies, 50 μ g ml⁻¹ (in ddH₂O) methylated BSA (Sigma-Aldrich) was added into wells of 96-well plates to incubate at 37 °C for 1 h, followed by the addition of 10 μ g ml⁻¹ (in PBS) pre-treated calf thymus DNA (Invitrogen, Carlsbad, CA, USA) to continue incubation at 4 °C overnight. Of note, the calf thymus DNA was pre-treated with S1 nuclease (Thermo Scientific, Waltham, MA, USA) to degrade single-stranded DNA. Plates were then washed three times with PBS-T and incubated with BlockPROTM blocking buffer

(Visual Protein, Taipei, Taiwan) at room temperature for 2 h. Mouse serum samples were diluted as indicated in brackets for IgG (1:200 000), IgM (1:15 000) and anti-dsDNA IgM (1:100). Standard curves of Ig were generated using a panel of known amounts of mouse IgG or IgM for quantification. Horseradish peroxidase (HRP)-conjugated rabbit anti-mouse IgG, Fcγ-specific or μ-specific goat anti-mouse IgM Abs were added for incubation at room temperature for 1 h, followed by development with tetramethylbenzidine substrate (BD Biosciences). To quench the reaction, 2 N H₂SO₄ was added. Plates were read at OD₄₅₀ nm and OD₅₇₀ nm using an enzyme-linked immunosorbent assay reader (BioTek, Winooski, VT, USA). The OD₄₅₀ minus OD₅₇₀ was calculated to determine the background of each well.

Enzyme-linked immunospot assay

Ninety-six-well HTS filter plates were treated as described for the enzyme-linked immunosorbent assay for detection of mouse IgG, IgM and dsDNA Ab levels. RPMI 1640 medium was added to each well of the plates before adding cells (2.0×10^4 cells per well and 1.6×10^5 per well for detection of IgG and IgM, respectively, with two-fold serial dilutions) for incubation at 37 °C overnight. Plates were washed with PBS-T, followed by addition of HRP-conjugated goat Abs specific for human μ or γ chain (1:5000) at room temperature for 1 h. After vigorous washes, spots were developed by the addition of 50 μl per well of 3-amino-9-ethylcarbazole substrate (BD Biosciences) for 20–30 min. Plates were scanned to enumerate spots using C.T.L. ImmunoSpot scanner and software (version 5.0.2).

Blood and biochemistry analysis

Serum creatinine was measured using a Roche Cobas C111 Chemistry Analyzer (Roche Diagnostics). Complete blood counts (CBCs) were analyzed using an IDEXX ProCyt Dx Hematology Analyzer (IDEXX Laboratories).

Immunohistochemistry examination

Adjacent sections of spleen were incubated with either B220 or FcγRIIB Ab at 4 °C overnight, according to the manufacturers' instructions. After washes with PBS-T, species-specific biotinylated mAbs were added at room temperature for 1 h, followed by avidin/biotinylated HRP at room temperature for 40 min. Slides were washed thoroughly before adding 3,3'-diaminobenzidine substrates for development. Sections were counterstained with hematoxylin before mounting. An Axioplan 2 light microscope (Zeiss, Oberkochen, Germany) was used to image sections. Images of representative splenic and renal sections with magnification of $\times 200$ were acquired for analysis. Four-μm thick paraffin-embedded kidney sections were stained with hematoxylin and eosin (H&E). The degree of deposition of ICs in the renal glomeruli was determined by staining with HRP-conjugated rabbit anti-mouse IgG and goat anti-mouse IgM at room temperature for 1 h. Masson's trichrome staining was applied to detect collagen for measurement of fibrosis in kidneys. MetaMorph software (Molecular Devices, Sunnyvale, CA, USA) was used to quantify stained areas.

Transient transfection and *Fcgr2b* promoter activity assay

For luciferase assays, each *Fcgr2b* promoter reporter plasmid pGL-3 (10 μg) was co-transfected with the renilla reference plasmid pRL-SV40 (0.5 μg) into 5×10^6 BJAB cells by a Neon electroporator, according to the manufacturer's instructions (Thermo Fischer). After 4 h of transfection, vehicle or resveratrol was added for incubation at

37 °C for 24 h. The luciferase activities were measured using the dual luciferase reporter assay system (Promega). Firefly luciferase activity was normalized to renilla luciferase activity to yield the relative luciferase activity. The sequences of putative NF-κB-binding sites at the -480 promoter region of the *Fcgr2b* gene were mutated from TGGAGTCCCC to TTCTGTCCGC in the -600 promoter construct (Genebank access no. AF433951).

Immunoprecipitation, western blotting and chromatin immunoprecipitation

BJAB B cells (5×10^6 per ml) with or without resveratrol treatment were lysed with RIPA buffer for standard western blotting using Abs specific to Sirt1, FcγRIIB (Santa Cruz), p65 NF-κB, acetylated-p65 NF-κB (K310), p65 NF-κB (S536), p65 NF-κB (S468) and β-actin (Cell Signaling Technology, Danvers, MA, USA). Immunoprecipitation was performed using 4 μg phosphor-p65 NF-κB (S536) or phosphor-p65 NF-κB (S468), which were separately incubated with 500 μg of pre-cleared whole cell lysates overnight before SDS-PAGE and western blotting. Four micrograms of each p65 NF-κB, phosphor-p65 NF-κB (S536), phosphor-p65 NF-κB (S468) and acetylated p65 NF-κB (K310) Abs (Cell Signaling) were used for chromatin immunoprecipitation. PCR was performed using sequence-specific primers to amplify the -600 to -300 promoter region of the *Fcgr2b* gene.

Statistical analysis

Statistical analysis was performed using two-tailed unpaired Student's *t*-test. Graphs and histograms were plotted using GraphPad Prism 6.0 (GraphPad Software, San Diego, CA, USA). The survival rate of mice was analyzed each week by the log-rank (Mantel-Cox) test. The *t*-test was modified by Welch's correction in case of unequal variance. All results were shown as the mean \pm s.e. **P*<0.05, ***P*<0.01 and ****P*<0.001 denote degrees of statistical significance between two groups. NS indicates no significance.

RESULTS

Resveratrol treatment prolongs survival of MRL/*lpr* mice with full-blown disease

To evaluate the therapeutic effects of resveratrol, we divided 17-week-old MRL/*lpr* mice into vehicle (control) and resveratrol treatment groups. At this age, they exhibit an increased titer of serum anti-dsDNA autoantibodies and overt proteinuria owing to chronic glomerulonephritis. Without therapeutic intervention, approximately half of mice can die of renal failure at 24 weeks of age.²⁶ To conduct the experiments, either vehicle or resveratrol at a dose of 20 mg kg⁻¹ per day, which is equivalent to 1.62 mg kg⁻¹ per day in humans,²⁷ was given 10 times every other day intra-peritoneally. After the initiation of therapy, the survival of mice was monitored every week for 6 weeks (Figure 1a). As illustrated in Figure 1b, the number of live MRL/*lpr* mice was significantly higher in the resveratrol-treated group (33 out of 34) compared to vehicle-treated mice (15 out of 20) (*P*=0.0142) after 3 weeks of treatment. Moreover, most resveratrol-treated mice (32 out of 34) remained alive even 3 weeks after the cessation of treatment. By contrast, the survival rate of control mice considerably declined to 60% (12 out of 20, *P*=0.0016) (Figure 1b). These data indicate that resveratrol treatment can significantly extend the lifespan of full-blown MRL/*lpr* mice. Moreover, the lupus-

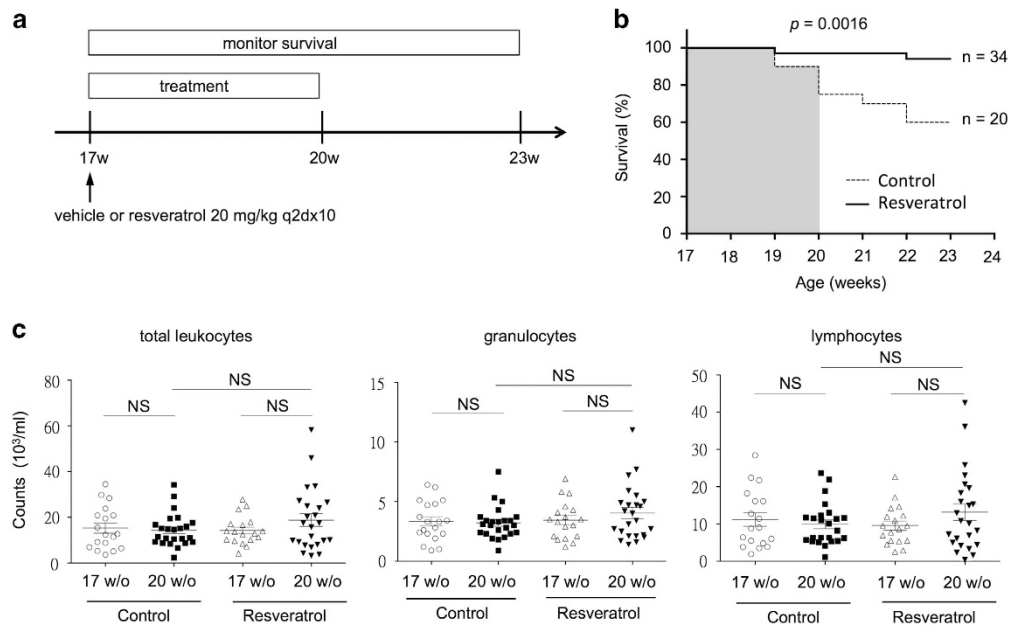


Figure 1 Resveratrol treatment prolongs the survival of MRL/lpr mice. (a) A schematic illustration of the treatment protocol for MRL/lpr mice at 17 weeks of age when renal pathology is evident.²⁸ Intra-peritoneal administration of either vehicle (olive oil) or resveratrol at 20 mg kg⁻¹ to mice was conducted ten times every other day. (b) Survival rates of control (dash line, $n=34$) and resveratrol-treated (solid line, $n=20$) mice during the treatment period (17–20 weeks of age) were analyzed using the log-rank (Mantel–Cox) test ($P=0.0142$). After the cessation of treatment, the number of live mice was continuously monitored and documented for comparisons between the control and resveratrol-treated groups for an additional three weeks. The survival rates of mice in these two groups were plotted and compared ($P=0.0016$) as in b. (c) Comparisons of the numbers of total leukocytes (white blood cells), granulocytes and lymphocytes in the peripheral blood between vehicle ($n=19$) and resveratrol ($n=24$)-treated MRL/lpr mice.

like symptoms of mice, including patches of fur loss, skin rash and loss of whiskers, were markedly improved in the resveratrol-treated group (Supplementary Figure 1). To determine the effects of resveratrol on immune cells, we investigated the vehicle- and resveratrol-treated mice in detail at the endpoint of therapy. Consistently, the numbers of total leukocytes (Figure 1c, left), granulocytes (Figure 1c, middle) and lymphocytes (Figure 1c, right) in circulation were unaffected.

Resveratrol treatment improves splenomegaly and decreases the numbers of splenic germinal center B cells and bone marrow B cells

In the resveratrol-treated group, splenomegaly was significantly improved by an ~30% decrease in size, suggesting reduced cell expansion or infiltration (Figure 2a). We next examined the immune cells in the peripheral blood, spleen and bone marrow using flow cytometry. As shown in Figure 2b, the number of CD19⁺ B cells in the spleen and bone marrow, but not in the blood, was significantly reduced. Interestingly, we found that splenic CD19⁺GL7⁺ germinal center (GC) B cells were also substantially decreased (Figure 2c). By contrast, the populations of T cells (Figure 2d), CD11b⁺ myeloid (Figure 2e) and CD11c⁺ dendritic cells (Figure 2f) in the spleen were unaltered.

Resveratrol treatment reduces splenic and bone marrow PC numbers and serum autoantibodies in MRL/lpr mice

After observing the beneficial effects of resveratrol in the SLE phenotype and decreased B-cell numbers in the bone marrow

and germinal center, we then examined whether resveratrol treatment could reduce the number of PCs. Enzyme-linked immunospot assays, which can detect PCs at the single-cell level, were performed to quantify the numbers of PCs in the spleen and bone marrow. We found that after resveratrol treatment, the number of PCs that secreted anti-dsDNA autoantibodies were significantly reduced by more than 50% in the spleen ($P=0.0236$) and in the bone marrow ($P=0.0148$), where long-lived PCs reside²⁸ (Figure 3a). To a similar extent, the IgG-secreting PCs were markedly decreased in the spleen ($P=0.0366$) and bone marrow ($P=0.0006$) (Figure 3b). Interestingly, the IgM-secreting PCs were more negatively affected by resveratrol treatment in the bone marrow ($P=0.0165$) than in the spleen ($P=0.168$) (Figure 3c).

Because PCs were drastically inhibited by resveratrol treatment, we next determined whether this effect could subsequently lead to a decreased level of serum autoantibodies. Indeed, resveratrol treatment significantly reduced serum IgG to a level lower than that prior to treatment ($P=0.0282$), whereas the serum IgG titer continued to increase as the disease progressed in control ($P=0.0013$) mice (Figure 4a). Moreover, as a result of reduced autoreactive PCs in the spleen and bone marrow, the serum titer of anti-dsDNA autoantibodies was significantly decreased by resveratrol treatment ($P=0.0221$) (Figure 4b). By contrast, the levels of circulating IgM were not significantly altered in the control or resveratrol-treated groups (Figure 4c).

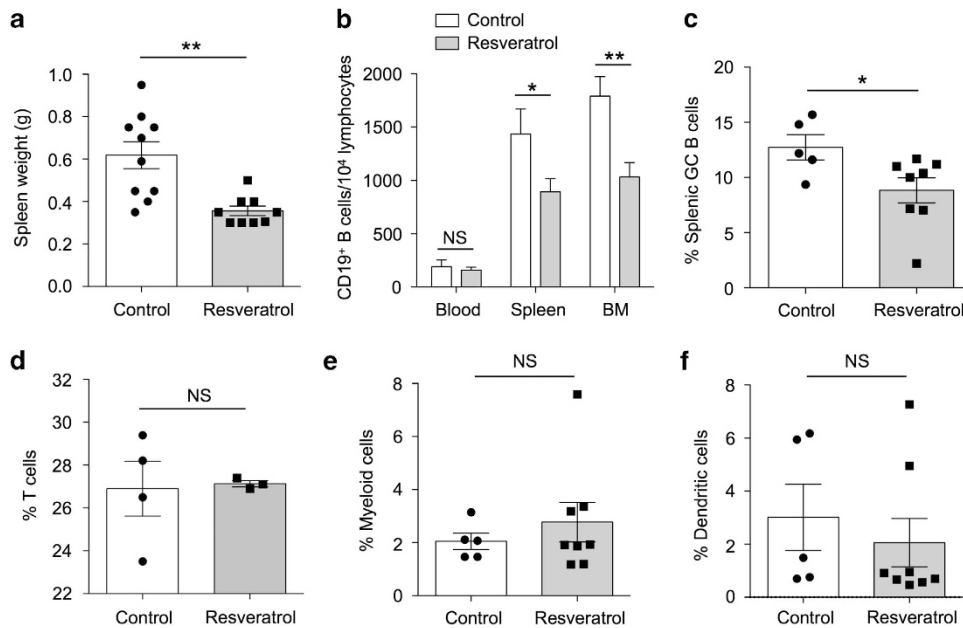


Figure 2 Resveratrol treatment decreases B cells in the bone marrow of MRL/lpr mice. (a) The weight of spleens of MRL/lpr mice from control and resveratrol-treated groups was measured and compared after the completion of treatment at 20 weeks of age ($P=0.0024$). The percentages of (b) CD19⁺ B cells (control, $n=6$; resveratrol-treated, $n=8$) in the blood, spleen and bone marrow (BM) ($P=0.6634$, 0.0479 and 0.0071, respectively) and (c) CD19⁺GL7⁺ germinal center (GC) B cells in the spleen between control ($n=10$) and resveratrol-treated ($n=9$) groups were quantified by flow cytometry, compared and are presented as bar graphs ($P=0.0458$). The percentages of (d) CD3⁺ T cells ($P=0.8675$), (e) CD11b⁺ myeloid cells and (f) CD11c⁺ dendritic cells in the spleen were measured for comparison between control and resveratrol-treated groups. Data from control and resveratrol-treated mice are shown as the mean \pm s.e.m. * $P<0.05$ and ** $P<0.01$ denote statistical significance, whereas NS indicates no significance.

Resveratrol treatment ameliorates lupus nephritis and disease onset in MRL/lpr mice

Because resveratrol treatment significantly reduced the number of PCs as well as the titers of serum autoantibodies, we investigated whether chronic lupus nephritis could be improved in MRL/lpr mice. Indeed, we detected a marked decrease of lupus nephritis-induced fibrosis after resveratrol treatment, as measured by Masson's trichrome staining for collagen deposition (Figure 5a, left). As lupus nephritis is characterized by glomerular and tubulo-interstitial inflammation followed by progressive fibrosis of glomerulus (glomerulosclerosis) and interstitial fibrosis between tubules, we quantified collagen deposition at these regions. Both glomerular and tubulo-interstitial fibrosis was significantly reduced by ~50% in response to resveratrol treatment (Figure 5a, right). Consistent with the alleviation of fibrotic changes in the glomerular areas, the accumulation of both IgG- and IgM-ICs in the glomeruli was significantly diminished in resveratrol-treated mice (Figure 5b). In addition, because normal renal tubules express low levels of Sirt1,²⁹ we investigated whether tubular Sirt1 could be up-regulated by resveratrol. As shown in Figure 5c, the expression levels of Sirt1 in renal tubules were already substantially increased in control mice; nevertheless, resveratrol treatment further enhanced tubular expression of Sirt1. Correspondingly, the expression of acetylated p65 NF- κ B (K310) in renal tubules was significantly reduced in resveratrol-treated mice. As a result of improved glomerular pathology and enhanced tubular protection, the serum level of creatinine,

which is cleared via excretion into urine, was markedly decreased in resveratrol-treated mice compared to the control group ($P=0.037$) (Figure 5d).

Resveratrol upregulates the surface expression of FcγRIIB on B cells and myeloid cells

To determine whether the reduction of B cells by resveratrol is associated with FcγRIIB-mediated inhibition, we examined the expression levels of FcγRIIB in B cells in lymphoid compartments of vehicle- and resveratrol-treated MRL/lpr mice. We found that the surface expression levels of FcγRIIB on B cells in the spleen (Figure 6a, $P=0.0219$), including the GC B cells (Figure 6b, $P=0.035$), were significantly enhanced by ~20–30% after resveratrol treatment as determined by flow cytometry. Likewise, in the bone marrow, the surface expression of FcγRIIB on B cells (Figure 6c, $P=0.0489$), including PCs (Figure 6d, $P=0.0487$), was upregulated to a similar degree. Interestingly, the expression level of FcγRIIB on splenic myeloid cells (Figure 6e, $P=0.0457$), but not dendritic cells (Figure 6f), was also increased. Consistently, the expression levels of FcγRIIB in B220⁺ B-cell follicles were significantly increased after resveratrol treatment as determined by immunohistochemical examination (Figure 6g and h).

Resveratrol increases the gene expression of FcγRIIB in B cells via NF- κ B-dependent promoter activation

To investigate the molecular mechanisms of FcγRIIB up-regulation by resveratrol, BJAB B cells were used for detailed

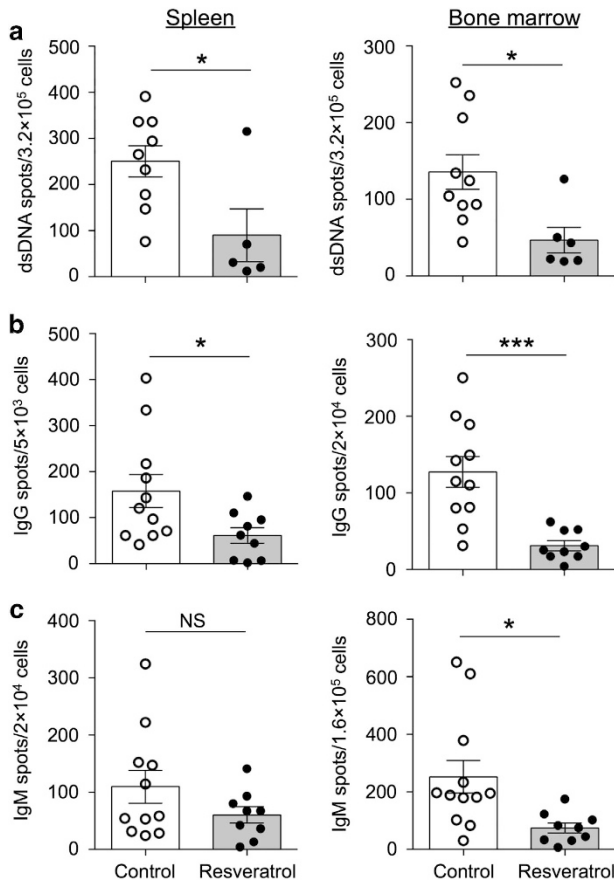


Figure 3 Resveratrol treatment reduces the numbers of plasma cells (PCs) in the spleen and bone marrow of MRL/*lpr* mice. Enzyme-linked immunospot (ELISPOT) assays to quantify the numbers of PCs of (a) dsDNA-PCs, (b) IgG-PCs and (c) IgM-PCs in the spleen (left, 5×10^3 splenocytes) and bone marrow (right, 2×10^4 bone marrow (BM) cells) of control (empty circle) and resveratrol-treated (solid circle) MRL/*lpr* mice. * $P < 0.05$, *** $P < 0.001$, NS indicates no significance.

studies. Consistent with the findings *in vivo*, resveratrol treatment increased the expression levels of FcγRIIB in a concentration- and time-dependent manner (Figure 7a). In addition, the expression of Sirt1 was increased, with a concurrent decrease of p65 NF-κB (K310). To further determine the molecular mechanisms for resveratrol-induced FcγRIIB expression, we performed luciferase reporter assays to assess various promoter regions of -796, -600 and -471 bp upstream of the FcγRIIB gene start site. As shown in Figure 7b, resveratrol treatment induced up-regulation of the -796 and -600 bp, but not the -471 bp, promoter activities of the FcγRIIB gene. This result suggests the presence of a crucial regulatory element within the -600 and -471 region that is required for the resveratrol-dependent up-regulation of FcγRIIB. To elucidate the responsible factors, we used the JASPAR database to predict and map the binding sites for transcription factors in this region. As a result, a sole putative binding site for NF-κB was predicted within the -600 to -471 region (Figure 7c).

To further understand the role of NF-κB in the control of FcγRIIB transcription in response to resveratrol, we determined the expression level and activation status of NF-κB under resveratrol treatment. As previously reported,³⁰ we found that resveratrol treatment resulted in an increased expression of Sirt1 in BJAB B cells (Figure 7a). Because resveratrol is well known to deacetylate p65 NF-κB specifically at lysine 310 via Sirt1,⁸ we examined the roles of Sirt1 and p65 NF-κB in the regulation of FcγRIIB gene expression. First, we found a transient and concentration-dependent induction of Sirt1 by resveratrol after 2 h of treatment. Notably, the levels of total and acetylated p65 NF-κB at lysine 310 were markedly decreased in B cells (Figure 7a). Second, we mutated this binding site to determine whether p65 NF-κB is responsible for the resveratrol-induced upregulation of FcγRIIB gene transcription. Indeed, loss of the NF-κB binding site at the -480 region resulted in abrogation of resveratrol-mediated induction of FcγRIIB gene transcription (Figure 7d).

Because the transactivation activity of NF-κB depends on the acetylation and phosphorylation status of p65 NF-κB,³¹ we performed chromatin immunoprecipitation assays to determine the association of acetylated and phosphorylated p65 NF-κB proteins at the FcγRIIB promoter in response to resveratrol treatment in BJAB B cells. We focused on acetylated p65 NF-κB (K310) and phosphorylated p65 NF-κB (S536), as they are both important for promoting gene expression of pro-inflammatory cytokines,³² as well as phosphorylated p65 NF-κB (S468), as it may serve as a transcriptional repressor.^{33,34} The chromatin immunoprecipitation data revealed increased binding of total p65 NF-κB and phosphor-p65 NF-κB (S536) to the FcγRIIB promoter, which was accompanied by a reduced association of phosphor-p65 NF-κB (S468) and acetylated p65 NF-κB (K310) with this promoter region after resveratrol treatment (Figure 7e). Moreover, because both acetylation and phosphorylation of p65 NF-κB are known to influence its ability to bind target DNA sequences,³¹ we examined the acetylation status at lysine 310 of phosphor-p65 NF-κB proteins. We found that the lysine 310 residues of phosphor-p65 NF-κB (S536) were readily deacetylated after 30 min of resveratrol treatment; the deacetylation remained detectable at 2 h, whereas the acetylated lysine 310 of phosphor-p65 NF-κB (S468) was not considerably altered in the same period of treatment (Figure 7f). These results suggest that the deacetylated phosphor-p65 NF-κB (S536) proteins associate with the promoter sequences of *Fcgr2b* to enhance transcriptional activity.

DISCUSSION

In this study, we showed that resveratrol treatment can ameliorate lupus nephritis in MRL/*lpr* mice by upregulating FcγRIIB, leading to a selective reduction of B cells in the spleen and bone marrow (Figure 2). Because excess ICs are readily present in mice with full-blown lupus, enhanced expression of FcγRIIB in B cells can promote the triggering of FcγRIIB for inhibition (Figure 6). Moreover, PCs express the highest levels of FcγRIIB among B-cell subpopulations, and this renders

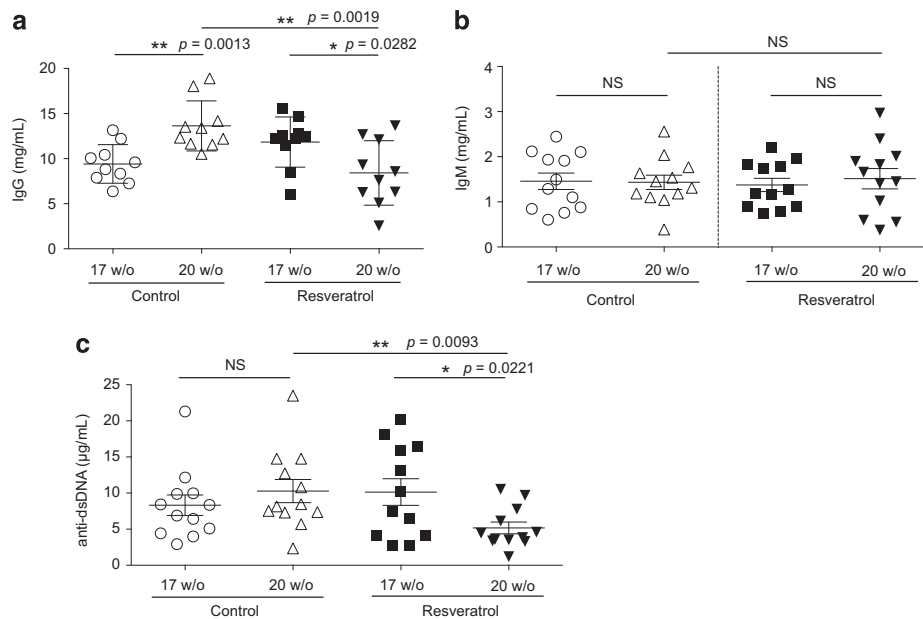


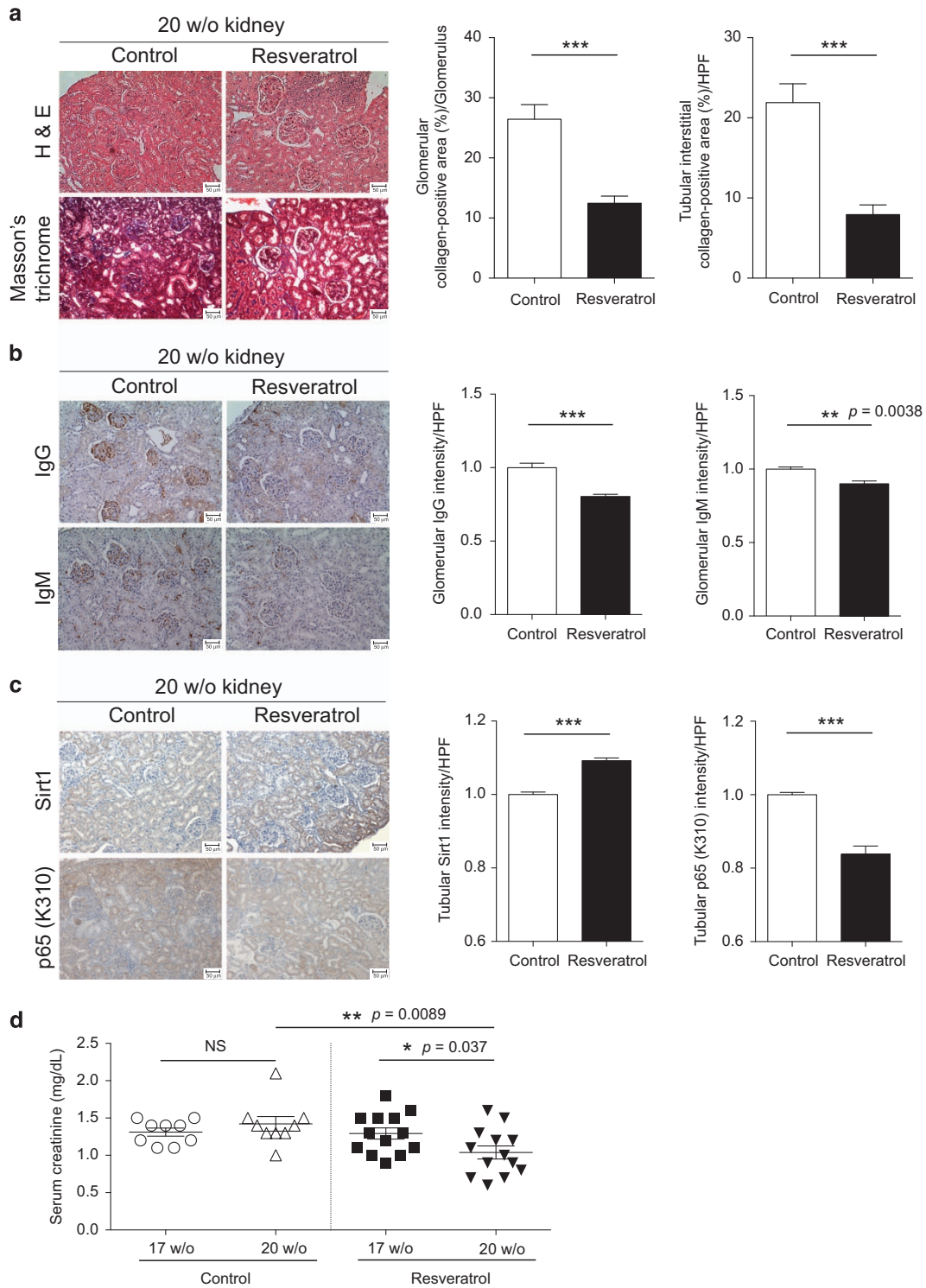
Figure 4 Resveratrol treatment reduces the serum levels of autoantibodies in MRL/lpr mice. Before (17 weeks of age) and after (20 weeks of age) treatment, serum levels of (a) total IgG, (b) total IgM and (c) anti-dsDNA of control ($n=10-12$) and resveratrol-treated ($n=10-12$) MRL/lpr mice were determined by enzyme-linked immunosorbent assay. Mouse sera were diluted for total IgG (1:200 000), total IgM (1:15 000) and anti-dsDNA IgM (1:100). * $P<0.05$, ** $P<0.01$, NS indicates no significance.

them most sensitive to FcγRIIB-mediated inhibition. As a consequence, PCs are the most significantly reduced in both the spleen and the bone marrow in response to resveratrol (Figure 3). Consistent with our findings, FcγRIIB was previously reported to regulate the apoptosis of PCs.^{17,24,25} Moreover, depletion of autoreactive PCs results in reduced autoantibody production, thereby leading to decreased IC deposition in the kidney (Figures 4 and 5). Thus, the survival of full-blown MRL/lpr mice was prolonged after resveratrol treatment (Figure 1).

In response to resveratrol treatment, the upregulation of FcγRIIB gene expression depends on increased binding of p65 NF-κB (S536) to the -480 region of the FcγRIIB promoter in B cells because mutation of this binding site abolished sensitivity to resveratrol (Figure 7). This result is consistent with a transactivation role for p65 NF-κB (S536) for gene expression.³⁰ However, we found decreased binding of deacetylated p65 NF-κB (K310) to the -480 promoter region of FcγRIIB. Interestingly, the acetylation status of p65 NF-κB at lysine 310 of S536-phosphorylated proteins was markedly decreased, but it remained stable in the S468-phosphorylated proteins after resveratrol treatment. Taken together, we reason that the association of deacetylated p65 NF-κB (S536) with the *Fcgr2b* promoter is increased in response to resveratrol, which leads to an up-regulation of FcγRIIB gene transcription in B cells (Figure 7e). Similar to our findings, deacetylation of p65 NF-κB (K122/123) by HDAC3 has been reported to enhance its ability for DNA binding.³³ Moreover, p65 NF-κB (S468) is considered to play a negative role in the control of gene transcription.^{31,35} Because resveratrol appeared to increase the expression level of p65 NF-κB (S468) while decreasing its

association with the *Fcgr2b* promoter (Figure 7a), we reason that p65 NF-κB (S468) might otherwise negatively regulate distinct genes, for example, B-cell activation genes. One caveat is that although the phosphorylation of p65 NF-κB on serine 536 is able to regulate the acetylation of lysine 310,³² whether the acetylation or deacetylation of lysine 310 could conversely directly affect the phosphorylation of p65 NF-κB on serine 536 and/or serine 468 is not yet known. Nevertheless, changes in the phosphorylation of p65 NF-κB (S536 and S468) were detected in the presence of deacetylation of lysine 310 by resveratrol in B cells (Figure 7). Other examples of immunosuppressive and inhibitory molecules include IL-10, TGF-β1 and indoleamine 2,3-dioxygenase gene promoters, in which p65 NF-κB is recruited for transcriptional regulation.^{36,37}

A significant reduction of anti-dsDNA PCs via FcγRIIB upregulation (Figure 3) is of great importance because bone marrow autoreactive PCs are major contributors to IC-mediated lupus nephritis. These PCs are likely substantially reduced from an early time point in response to resveratrol because the serum titers of anti-dsDNA Abs may persist in circulation for weeks and therefore decline to a comparable extent (Figure 4). In support of our findings, Hiepe and Radbruch³⁸ have recently demonstrated and emphasized that effective depletion of autoreactive PCs from the bone marrow is an important key to cure SLE because the bone marrow is the major site for PCs resistant to conventional therapies, for example, high-dose corticosteroid.^{39,40} This finding is of clinical importance because neither anti-proliferative agents, for example, cyclophosphamide, nor anti-CD20 mAbs, for example, rituximab, can effectively eliminate PCs in the bone marrow of SLE patients.^{38,41} Our data also indicate that the



upregulation of FcγRIIB by resveratrol can reduce bone marrow PCs irrespective of their surface Ig isotypes (Figure 3). In addition to PCs, we found that GC B cells in the spleen were sensitive to FcγRIIB-mediated inhibition (Figure 2c). The link between FcγRIIB and GC B cells has been proposed in the elimination of self-reactive B cells in GCs.⁴²⁻⁴⁴ In lupus-prone mice, a low expression level of FcγRIIB in GC B cells has been attributed to a failure to be

upregulated.¹⁹ Accordingly, enhanced FcγRIIB expression in B cells by resveratrol may facilitate the reduction of GC B cells in MRL/lpr lupus mice. Because GC B cells, if positively selected by Ag, can undergo proliferation and differentiation into PCs, the resultant decrease of PCs by resveratrol may be in part a consequence of decreased numbers of GC B cells.

In addition to B cells, the surface FcγRIIB level on myeloid cells was also increased by resveratrol (Figure 6e). However, the

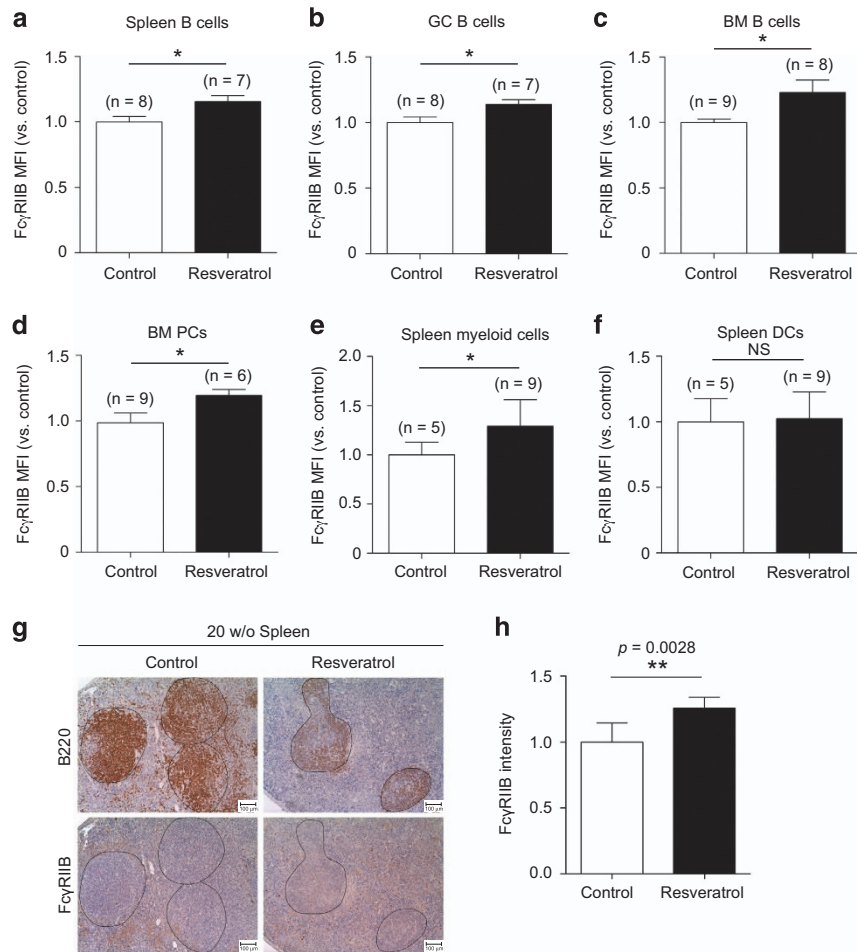
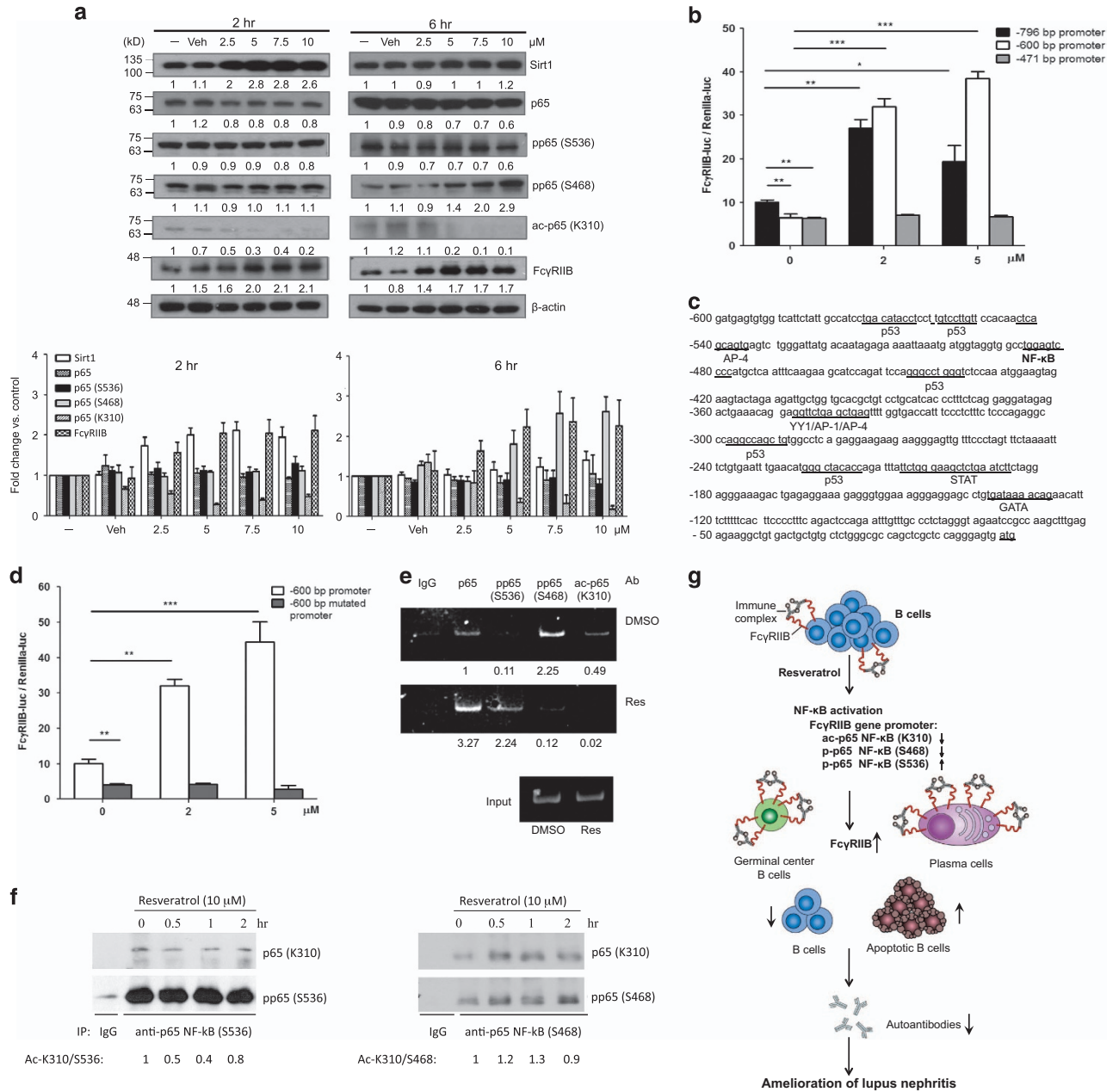


Figure 6 Resveratrol treatment enhances the surface expression of FcγRIIB on B cells. Bar graphs of flow cytometry analyses on the expression levels of FcγRIIB of (a) total splenic CD19⁺ B cells ($P=0.0219$) and (b) Germinal center (GC) B cells ($P=0.035$) between control ($n=8$) and resveratrol-treated ($n=7$) groups. Bar graphs to compare the mean fluorescence intensity (MFI) of FcγRIIB expression on (c) CD19⁺ B cells ($P=0.0489$) and (d) PCs ($P=0.0487$) in the bone marrow between control ($n=9$) and resveratrol-treated ($n=8$) groups. Bar graphs of flow cytometric quantification to compare the MFI of FcγRIIB on splenic (e) CD11b⁺ myeloid cells ($P=0.0457$) and (f) CD11c⁺ dendritic cells between control ($n=5$) and resveratrol-treated ($n=9$) groups. The MFI levels of FcγRIIB on cells were shown as the fold changes with respect to levels in the control. (g) Immunohistological examination and (h) quantification of the intensity (expression level) of FcγRIIB in B220⁺ B cells (circled regions) in follicles (>15 follicles per section) between control and resveratrol-treated mice. Scale bars denote 50 μm. Quantification results are illustrated in a bar graph. * $P<0.05$, ** $P<0.01$.

Figure 5 Resveratrol treatment ameliorates lupus nephritis and reduces fibrosis and immune complex (IC) deposition in the kidneys of MRL/lpr mice. (a) Kidneys from control ($n=4$) and resveratrol-treated ($n=4$) MRL/lpr mice were sectioned and stained with H&E and Masson's trichrome solutions. Sections of collagen-positive areas (shown in blue) revealed by Masson's trichrome staining were quantified as the average percentage of each high-power field (HPF) (>5 HPFs/section/mouse, >6 glomeruli/HPF) using MetaMorph software for control ($n=4$) and resveratrol-treated ($n=4$) MRL/lpr mice. Areas of collagen-deposition at the glomerular and tubulo-interstitial space were quantified separately. (b) Deposition of IgG- and IgM-ICs in the glomeruli on renal sections of control ($n=3$) and resveratrol-treated ($n=3$) MRL/lpr mice. Three mouse kidneys of each group were analyzed. Quantification was performed, analyzed and presented as in a. (c) Sections of control ($n=3$) and resveratrol-treated ($n=3$) mice were stained and quantified for the expression of Sirt1 and p65 NF-κB (K310) as in a. (d) Before (17 weeks of age) and after (20 weeks of age) treatment, serum creatinine levels were measured by enzyme-linked immunosorbent assay to compare control ($n=9$) and resveratrol-treated ($n=13$) mice. Scale bars, 50 μm. * $P<0.05$, ** $P<0.01$, *** $P<0.001$.



number of myeloid cells in the spleen was not affected by resveratrol treatment (Figure 2e). This result is because FcγRIIB mediates apoptosis only in B cells and not in other immune cells.^{17,34,42,45} Meanwhile, it has been demonstrated that overexpression of FcγRIIB in CD68⁺ macrophages has no effect on immune responses or protection against autoimmunity. By contrast, overexpression of FcγRIIB in B cells confers protective effects on the disease onset and resolution of SLE in mice.⁴⁶ Consistent with these results, retroviral transduction of ~40% of bone marrow B cells to express FcγRIIB was able to substantially decrease autoantibody production and improve nephropathy in lupus-prone mice.⁴⁷

A practical issue that limits the clinical use of resveratrol is its low oral bioavailability *in vivo*.⁴⁸ Nevertheless, our study showed that intra-peritoneal injection of 20 mg kg⁻¹ per day

was effective to confer selectivity to reduce B cells and alleviate the pathology of lupus nephritis in MRL/*lpr* mice (Figure 5). Consistent with our findings, Wang *et al.*⁴⁹ demonstrated that either 50 or 75 mg kg⁻¹ of oral resveratrol daily for 7 months can effectively suppress the activation of B cells and CD4⁺ T cells and reduce their cell numbers, leading to delayed development of pristane-induced lupus nephritis. In addition, our results indicate that B cells are more vulnerable to elimination by resveratrol in that a lower dose (20 mg kg⁻¹) of resveratrol appears to upregulate FcγRIIB expression in B cells to confer therapeutic benefits to lupus. By contrast, at least 10-fold higher doses are required to directly induce apoptosis of leukemic cells.⁵⁰

It is well established that Sirt1 is the key mediator for the action of resveratrol.^{6,7} Although Sirt1 can deacetylate and

inhibit many substrates that activate pro-inflammatory molecules, its role in the regulation of immune inhibitory molecules is less defined. It has been shown that resveratrol increases the expression of Sirt1 and down-regulates the levels of p65 NF-κB.^{30,51} Moreover, resveratrol activates Sirt1 to deacetylate p65 NF-κB.⁸ We showed that Sirt1 was induced by resveratrol to inhibit B cells and ameliorate SLE in a mouse model with constitutive and continued activation of Th1 cells. Consistently, Sirt1 activation by resveratrol has been shown to inhibit autoantibody production and B-cell proliferation.⁴⁹ In the regulation of FcγRIIB gene expression, we showed that enhanced binding of p65 NF-κB (S536) but dissociation of deacetylated p65 NF-κB (K310) to the -480 promoter region of FcγRIIB gene was important for the resveratrol-mediated upregulation of FcγRIIB expression (Figure 7g). By contrast, the acetylation of p65 NF-κB (K310) is known to be regulated by preceding phosphorylation of serine 536, and such phosphorylated and acetylated forms of p65 NF-κB enhance the transcriptional activities of pro-inflammatory genes.^{28,30} Our data provide a causal relationship between Sirt1 activation and FcγRIIB upregulation in B cells in response to resveratrol. In addition, FcγRIIB Sirt1 is an SLE susceptible gene,¹¹ and Sirt1 was implicated in the pathology of MRL/lpr mice.⁵² Similar to the phenotype of FcγRIIB knockout mice, Sirt1 deficiency results in the development of an autoimmune syndrome in mice, including autoantibody production and IC-mediated glomerulonephritis.⁹

Lupus nephritis is characterized by glomerular and tubulo-interstitial inflammation and mesangial cell proliferation, followed by progressive fibrosis of the glomerulus (glomerulosclerosis) and interstitial fibrosis between tubules if not properly treated. As shown in Figure 5, resveratrol significantly reduced fibrosis in both the glomeruli and tubulo-interstitial space and substantially restored glomerular morphology.

Moreover, the degree of IC deposition in the glomerulus was markedly lessened. In diabetes mellitus and acute injury induced by ischemia and reperfusion, renal tubular Sirt1 was shown to have protective effects.^{29,53} Consistent with this finding, Sirt1 deficiency displays characteristic phenotypes of lupus nephritis in mice and in humans.^{9,11} In vehicle-treated MRL/lpr mice, we found an increased expression of tubular Sirt1 proteins (Figure 5c). This finding suggests a crucial, physiological role of Sirt1 in the protection of renal tubules. Moreover, because Sirt1 expression was predominantly enhanced in renal tubules by resveratrol (Figure 5c), the improvement of glomerular function in MRL/lpr mice is likely a consequence of reduced numbers of autoreactive B cells and thereby decreased deposition of ICs in the glomeruli (Figure 5b). This notion is further supported by the fact that autoantibodies can activate glomerular mesangial cells and promote their differentiation into myofibroblast-like cells, which produce collagen and extracellular matrix.⁵⁴

The inhibitory effects of enhanced FcγRIIB expression on B cells *in vivo* may allow FcγRIIB to execute a self-regulatory feedback loop to control the number of PCs via IC-dependent apoptosis. This effect is of clinical relevance in that reduced surface FcγRIIB expression on memory B cells and PCs is often observed in human SLE patients, leading to a limited capacity to restrain B cells from activation and to induce apoptosis of PCs.^{21–23} Here we provide evidence that the pharmacological upregulation of FcγRIIB expression by resveratrol can result in a significant decrease of PCs and autoantibody production, even though the underlying pathology of T cells persists, for example, in MRL/lpr mice. It has been shown that a chimeric Ab molecule that cross-links their DNA-reactive BCR with FcγRIIB can achieve a selective reduction of dsDNA-specific B cells. However, the PCs are resistant to this chimeric antibody.⁵⁵ This finding strongly supports the notion that the

Figure 7 Resveratrol upregulates the gene expression of Sirt1 and FcγRIIB and downregulates acetylated p65 NF-κB (K310) in B cells. (a) (Upper panel) BJAB B cells were treated without or with various concentrations (0, 2.5, 5, 7.5, 10 μM) of resveratrol for 2 h and 6 h. Cell lysates were prepared for western blotting to determine the levels of Sirt1, p65 NF-κB, acetylated p65 NF-κB, FcγRIIB and β-actin in response to resveratrol. A representative set of data from three independent experiments is illustrated (lower panel). Quantification was performed using ImageJ. Each target protein was normalized to its corresponding β-actin level and then to the sample without treatment. (b) The promoter regions of 796, 600 and 471 bp upstream to the transcription start site of *Fcgr2b* gene were linked to the firefly luciferase gene. BJAB B cells were co-transfected with each promoter construct and renilla luciferase gene, which served as an internal control for transfection efficiency. Resveratrol at 0, 2 or 5 μM was added for 24 h after transfection. (c) The activities of the 600 bp promoter construct containing either wild-type or the mutated NF-κB-binding site were assayed as in b. (d) Putative binding sites of transcription factors within the -600 region upstream of the transcriptional start site of the *Fcgr2b* gene. (e) BJAB B cells were treated in the absence or presence of 10 μM resveratrol for 4 h. Chromatin immunoprecipitation (ChIP) assays were performed to determine the binding of total and post-translationally modified p65 NF-κB (S536, S468 and K310) to the -600 to -471 bp promoter sequences. A representative of two independent experiments is shown. (f) BJAB B cells (2 × 10⁶ per ml) were treated with 10 μM resveratrol for 0, 0.5, 1 and 2 h. Cell lysates were subjected to immunoprecipitation with control rabbit IgG, p65 NF-κB (S468) or p65 NF-κB (S536) Abs, followed by western blotting with Abs specific to p65 NF-κB (K310). A representative of three independent experiments is shown. The K310 acetylation of phosphor-p65 NF-κB proteins upon resveratrol treatment was analyzed by quantifying the amounts of acetylated p65 NF-κB (K310) vs p65 NF-κB (S536 or S468), followed by normalization of respective results from various time points to that of untreated cells and presented as fold changes. (g) A schematic to illustrate that upregulation of FcγRIIB via p65 NF-κB by resveratrol selectively inhibits bone marrow plasma cells and splenic germinal center B cells to provide beneficial effects on the treatment of lupus nephritis. **P* < 0.05, ***P* < 0.01, ****P* < 0.001.

depletion of autoreactive PCs in the bone marrow after resveratrol treatment is mainly mediated by the FcγRIIB-dependent apoptotic pathway rather than inhibition of BCR-dependent activation.

There is growing evidence to support the theory that elimination of PCs, especially long-lived PCs in the bone marrow, is the key to curative treatment for SLE patients.^{38–41} Our data suggest that inhibition via FcγRIIB by resveratrol can reduce autoreactive PCs in the bone marrow. Clinically, upregulation of FcγRIIB in B cells will be of particular benefit for improving the outcome of SLE patients who manifest downregulation of surface FcγRIIB on their memory B cells and PCs.^{21–23} In addition, our study demonstrated that NF-κB is a critical regulator of resveratrol in the upregulation of FcγRIIB expression. Because neither T cells nor NK cells express FcγRIIB, the selective modulation on humoral immunity via FcγRIIB highlights a unique approach to treat SLE with little or no influence on other immune functions, thereby circumventing the side effects of systemic immunosuppression induced by current therapeutics, for example, corticosteroid and cyclophosphamide. Thus, FcγRIIB can be considered a therapeutic target for B-cell-mediated immunotherapy in autoimmune diseases.

CONFLICT OF INTEREST

The authors declare no conflict of interest.

ACKNOWLEDGEMENTS

This study was supported by research grants from the Ministry of Science and Technology of the Executive Yuan of Taiwan (NSC98-2320-B-002-056 and NSC99-2320-B-002-011). We thank Dr Wenyu Hsiao, Ms Wan-Yu Li, Ms Yu-Syuan You and Mr Tsung-Chih Tseng for their excellent technical support. We also acknowledge the service provided by the First Core Laboratory, College of Medicine, National Taiwan University.

- 1 Tsokos GC. Systemic lupus erythematosus. *N Engl J Med* 2011; **365**: 2110–2121.
- 2 Ugarte-Gil MF, Alarcón GS. Systemic lupus erythematosus: a therapeutic challenge for the XXI century. *Clin Rheumatol* 2014; **33**: 441–450.
- 3 Waibel M, Christiansen AJ, Hibbs ML, Shortt J, Jones SA, Simpson I *et al*. Manipulation of B-cell responses with histone deacetylase inhibitors. *Nat Commun* 2015; **6**: 6838–6849.
- 4 Zouali M. B lymphocytes—chief players and therapeutic targets in autoimmune diseases. *Front Biosci* 2008; **13**: 4852–4861.
- 5 Park EJ, Pezzuto JM. The pharmacology of resveratrol in animals and humans. *Biochim Biophys Acta* 2015; **1852**: 1071–1113.
- 6 Inoue H, Nakata R. Resveratrol targets in inflammation. *Endocr Metab Immune Disord Drug Targets* 2015; **15**: 186–195.
- 7 Han G, Xia J, Gao J, Inagaki Y, Tang W, Kokudo N. Anti-tumor effects and cellular mechanisms of resveratrol. *Drug Discov Ther* 2015; **9**: 1–12.
- 8 Yeung F, Hoberg JE, Ramsey CS, Keller MD, Jones DR, Frye RA *et al*. Modulation of NF-κB-dependent transcription and cell survival by the SIRT1 deacetylase. *EMBO J* 2004; **23**: 2369–2380.
- 9 Sequeira J, Boily G, Bazinet S, Saliba S, He X, Jardine K *et al*. Sirt1-null mice develop an autoimmune-like condition. *Exp Cell Res* 2008; **314**: 3069–3074.
- 10 Hu N, Qiu X, Luo Y, Yuan J, Li Y, Lei W *et al*. Abnormal histone modification patterns in lupus CD4⁺ T cells. *J Rheumatol* 2008; **35**: 804–810.
- 11 Consiglio CR, Juliana da Silveira S, Monticelio OA, Xavier RM, Brenol JC, Chies JA. SIRT1 promoter polymorphisms as clinical modifiers on systemic lupus erythematosus. *Mol Biol Rep* 2014; **41**: 4233–4239.
- 12 Espéli M, Smith KG, Clatworthy MR. FcγRIIB and autoimmunity. *Immunol Rev* 2016; **269**: 194–211.
- 13 Daeron M. Fc receptors as adaptive immunoreceptors. *Curr Top Microbiol Immunol* 2014; **382**: 131–164.
- 14 Chacko GW, Tridandapani S, Damen JE, Liu L, Krystal G, Coggeshall K. Negative signaling in B lymphocytes induces tyrosine phosphorylation of the 145-kDa inositol polyphosphate 5-phosphatase, SHIP. *J Immunol* 1996; **157**: 2234–2238.
- 15 Ono M, Bolland S, Tempst P, Ravetch JV. Role of the inositol phosphatase SHIP in negative regulation of the immune system by the receptor FcγRIIB. *Nature* 1996; **383**: 263–266.
- 16 Tzeng SJ, Bolland S, Inabe K, Kurosaki T, Pierce SK. The B cell inhibitory Fc receptor triggers apoptosis by a novel c-Abl family kinase-dependent pathway. *J Biol Chem* 2005; **280**: 35247–35254.
- 17 Tzeng SJ, Li WY, Wang HY. FcγRIIB mediates antigen-independent inhibition on human B lymphocytes through Btk and p38 MAPK. *J Biomed Sci* 2015; **22**: 87–98.
- 18 Bolland S, Ravetch JV. Spontaneous autoimmune disease in FcγRIIB-deficient mice results from strain-specific epistasis. *Immunity* 2000; **13**: 277–285.
- 19 Rahman ZS, Manser T. Failed up-regulation of the inhibitory IgG Fc receptor FcγRIIB on germinal center B cells in autoimmune-prone mice is not associated with deletion polymorphisms in the promoter region of the FcγRIIB gene. *J Immunol* 2005; **175**: 1440–1449.
- 20 Kelley JM, Edberg JC, Kimberly RP. Pathways: Strategies for susceptibility genes in SLE. *Autoimmun Rev* 2010; **9**: 473–476.
- 21 Isaák A, Gergely P Jr, Szekeres Z, Prechl J, Poór G, Erdei A *et al*. Physiological up-regulation of inhibitory receptors FcγRII and CR1 on memory B cells is lacking in SLE patients. *Int Immunol* 2008; **20**: 185–192.
- 22 Mackay M, Stanevsky A, Wang T, Aranow C, Li M, Koenig S *et al*. Selective dysregulation of the FcγRIIB receptor on memory B cells in SLE. *J Exp Med* 2006; **203**: 2157–2164.
- 23 Su K, Yang H, Li X, Li X, Gibson AW, Cafardi JM *et al*. Expression profile of FcγRIIB on leukocytes and its dysregulation in systemic lupus erythematosus. *J Immunol* 2007; **178**: 3272–3280.
- 24 Fukuyama H, Nimmerjahn F, Ravetch JV. The inhibitory Fcγ receptor modulates autoimmunity by limiting the accumulation of immunoglobulin G₊ anti-DNA plasma cells. *Nat Immunol* 2005; **6**: 99–106.
- 25 Xiang Z, Cutler AJ, Brownlie RJ, Fairfax K, Lawlor KE, Severinson E *et al*. FcγRIIB controls bone marrow plasma cell persistence and apoptosis. *Nat Immunol* 2007; **8**: 419–429.
- 26 Takahashi S, Fossati L, Iwamoto M, Merino R, Motta R, Kobayakawa T *et al*. Imbalance towards Th1 predominance is associated with acceleration of lupus-like autoimmune syndrome in MRL mice. *J Clin Invest* 1996; **97**: 1597–1604.
- 27 Blanchard OL, Smoliga JM. Translating dosages from animal models to human clinical trials—revisiting body surface area scaling. *FASEB J* 2015; **9**: 1629–1634.
- 28 Nutt SL, Hodgkin PD, Tarlinton DM, Corcoran LM. The generation of antibody-secreting plasma cells. *Nat Rev Immunol* 2015; **15**: 160–171.
- 29 Fan H, Yang HC, You L, Wang YY, He WJ, Hao CM. The histone deacetylase, SIRT1, contributes to the resistance of young mice to ischemia/reperfusion-induced acute kidney injury. *Kidney Int* 2013; **83**: 404–413.
- 30 Zhu X, Liu Q, Wang M, Liang M, Yang X, Xu X *et al*. Activation of Sirt1 by resveratrol inhibits TNF-α induced inflammation in fibroblasts. *PLoS ONE* 2011; **11**: e27081.
- 31 Christian F, Smith EL, Carmody RJ. The regulation of NF-κB subunits by phosphorylation. *Cells* 2016; **5**: pii: E12.
- 32 Chen LF, Williams SA, Mu Y, Nakano H, Duerr JM, Buckbinder L *et al*. NF-κB RelA phosphorylation regulates RelA acetylation. *Mol Cell Biol* 2005; **25**: 7966–7975.
- 33 Kiernan R, Brès V, Ng RW, Coudart MP, El Messaoudi S, Sardet C *et al*. Post-activation turn-off of NF-κB-dependent transcription is regulated by acetylation of p65. *J Biol Chem* 2003; **278**: 2758–2766.
- 34 Huang B, Yang XD, Lamb A, Chen LF. Posttranslational modifications of NF-κB: another layer of regulation for NF-κB signaling pathway. *Cell Signal* 2010; **22**: 1282–1290.
- 35 Buss H, Dörrie A, Schmitz ML, Frank R, Livingstone M, Resch K *et al*. Phosphorylation of serine 468 by GSK-3β negatively regulates basal p65 NF-κB activity. *J Biol Chem* 2004; **279**: 49571–49574.

- 36 Chang TP, Kim M, Vancurova I. Analysis of TGFβ1 and IL-10 transcriptional regulation in TCCL cells by chromatin immunoprecipitation. *Methods Mol Biol* 2014; **1172**: 329–341.
- 37 Ogasawara N, Oguro T, Sakabe T, Matsushima M, Takikawa O, Isobe K *et al*. Hemoglobin induces the expression of indoleamine 2,3-dioxygenase in dendritic cells through the activation of PI3K, PKC, and NF-κB and the generation of reactive oxygen species. *J Cell Biochem* 2009; **108**: 716–725.
- 38 Hiepe F, Radbruch A. Plasma cells as an innovative target in autoimmune disease with renal manifestations. *Nat Rev Nephrol* 2016; **12**: 232–240.
- 39 Hoyer BF, Moser K, Hauser AE, Peddinghaus A, Voigt C, Eilat D *et al*. Short-lived plasmablasts and long-lived plasma cells contribute to chronic humoral autoimmunity in NZB/W mice. *J Exp Med* 2004; **199**: 1577–1584.
- 40 Mumtaz IM, Hoyer BF, Panne D, Moser K, Winter O, Cheng QY *et al*. Bone marrow of NZB/W mice is the major site for plasma cells resistant to dexamethasone and cyclophosphamide: implications for the treatment of autoimmunity. *J Autoimmun* 2012; **39**: 180–188.
- 41 Mahévas M, Michel M, Weill JC, Reynaud CA. Long-lived plasma cells in autoimmunity: lessons from B-cell depleting therapy. *Front Immunol* 2013; **4**: 494–498.
- 42 Pearce RN, Kawabe T, Bolland S, Guinamard R, Kurosaki T, Ravetch JV. SHIP recruitment attenuates FcγRIIB-induced B cell apoptosis. *Immunity* 1999; **10**: 753–760.
- 43 Tiller T, Kofer J, Kreschel C, Busse CE, Riebel S, Wickert S *et al*. Development of self-reactive germinal center B cells and plasma cells in autoimmune FcγRIIB-deficient mice. *J Exp Med* 2010; **207**: 2767–2778.
- 44 Espéli M, Clatworthy MR, Bökers S, Lawlor KE, Cutler AJ, Köntgen F *et al*. Analysis of a wild mouse promoter variant reveals a novel role for FcγRIIB in the control of the germinal center and autoimmunity. *J Exp Med* 2012; **209**: 2307–2319.
- 45 McGaha TL, Karlsson MC, Ravetch JV. FcγRIIB deficiency leads to autoimmunity and a defective response to apoptosis in Mrl-MpJ mice. *J Immunol* 2008; **180**: 5670–5679.
- 46 Brownlie RJ, Lawlor KE, Niederer HA, Cutler AJ, Xiang Z, Clatworthy MR *et al*. Distinct cell-specific control of autoimmunity and infection by FcγRIIB. *J Exp Med* 2008; **205**: 883–895.
- 47 McGaha TL, Sorrentino B, Ravetch JV. Restoration of tolerance in lupus by targeted inhibitory receptor expression. *Science* 2005; **307**: 590–593.
- 48 Walle T, Hsieh F, DeLegge MH, Oatis JE Jr, Walle UK. High absorption but very low bioavailability of oral resveratrol in humans. *Drug Metab Dispos* 2004; **32**: 1377–1382.
- 49 Wang ZL, Luo XF, Li MT, Xu D, Zhou S, Chen HZ *et al*. Resveratrol possesses protective effects in a pristane-induced lupus mouse model. *PLoS ONE* 2014; **9**: e114792.
- 50 Ferry-Dumazet H, Garnier O, Mamani-Matsuda M, Vercauteren J, Belloc F, Billiard C *et al*. Resveratrol inhibits the growth and induces the apoptosis of both normal and leukemic hematopoietic cells. *Carcinogenesis* 2002; **23**: 1327–1333.
- 51 Pan W, Yu H, Huang S, Zhu P. Resveratrol protects against TNF-α-induced injury in human umbilical endothelial cells through promoting sirtuin-1-induced repression of NF-κB and p38 MAPK. *PLoS ONE* 2016; **11**: e0147034.
- 52 Zhang J, Lee SM, Shannon S, Gao B, Chen W, Chen A *et al*. The type III histone deacetylase Sirt1 is essential for maintenance of T cell tolerance in mice. *J Clin Invest* 2009; **119**: 3048–3058.
- 53 Hasegawa K, Wakino S, Simic P, Sakamaki Y, Minakuchi H, Fujimura K *et al*. Renal tubular Sirt1 attenuates diabetic albuminuria by epigenetically suppressing claudin-1 overexpression in podocytes. *Nat Med* 2013; **19**: 1496–1504.
- 54 Johnson RJ, Floege J, Yoshimura A, Iida H, Couser WG, Alpers CE. The activated mesangial cell: a glomerular 'myofibroblast'? *J Am Soc Nephrol* 1992; **2**: S190–S197.
- 55 Tchobanov AI, Voynova EN, Mihaylova NM, Todorov TA, Nikolova M, Yomtova VM *et al*. Selective silencing of DNA-specific B lymphocytes delays lupus activity in MRL/lpr mice. *Eur J Immunol* 2007; **37**: 3587–3596.



This work is licensed under a Creative Commons Attribution-NonCommercial-ShareAlike 4.0 International License. The images or other third party material in this article are included in the article's Creative Commons license, unless indicated otherwise in the credit line; if the material is not included under the Creative Commons license, users will need to obtain permission from the license holder to reproduce the material. To view a copy of this license, visit <http://creativecommons.org/licenses/by-nc-sa/4.0/>

© The Author(s) 2017

Supplementary Information accompanies the paper on Experimental & Molecular Medicine website (<http://www.nature.com/emm>)